

Design Methodology for Energy Efficient Unmanned Aerial Vehicles

Jingyu He¹, Yao Xiao¹, Paul Bogdan¹, and Corina Bogdan²

¹Department of Electrical Engineering, University of Southern California

²Department of Electrical and Computer Engineering, Northeastern University

Abstract— In this paper, we present a load-balancing approach to analyze and partition the UAV perception and navigation intelligence (PNI) code for parallel execution, as well as assigning each parallel computational task to a processing element in an Network-on-chip (NoC) architecture such that the total communication energy is minimized and congestion is reduced. First, we construct a data dependency graph (DDG) by converting the PNI high level program into Low Level Virtual Machine (LLVM) Intermediate Representation (IR). Second, we propose a scheduling algorithm to partition the PNI application into clusters such that (1) inter-cluster communication is minimized, (2) NoC energy is reduced and (3) the workloads of different cores are balanced for maximum parallel execution. Finally, an energy-aware mapping scheme is adopted to assign clusters onto tile-based NoCs. We validate this approach with a drone self-navigation application and the experimental results show that we can achieve up to 8.4x energy reduction and 10.5x performance speedup.

I. INTRODUCTION

Unmanned aerial vehicles (UAVs) are emerging as critical tools for mapping large areas, patrolling, searching, and rescuing applications. These tasks are usually dangerous, repetitive and have to be carried out in extreme conditions, making them ideal for autonomous drones. Self-navigation and collision-avoiding applications are key for UAVs to operate individually and rely on high-performance and low-power computing edges.

We cannot stress the importance of the performance of flight control applications enough. In a recent investigation [12], the Federal Aviation Administration discovered that the lack of data-processing speed of a specific flight control computer chip has led to two Boeing 737 Max crashes in 2019 that killed 346 people. At the same time, low-power design is critical for UAVs as well. One reason is that high power dissipation brings tremendous cooling challenges to maintain the hardware at a suitable temperature. Another is that batteries are the only energy source for drones, limiting the running time of drones.

In order to push the performance and energy boundary of systems-on-chips, Dally and Towles [7] proposed the tile-based Network-on-chips (NoC) as the ideal architecture for scalable and low-power on-chip communication. Such chips use tiles as building blocks such as CPUs, GPUs, ASIC and memory. A standard interface is embedded into each tile to route flits for communication. There have been many previous studies on energy-aware NoC designs. In contrast to prior NoC work, the goal of this paper is to investigate the parallelization of the UAV perception and navigation intelligence while taking the computation and communication power consumption into consideration. As shown in Fig. 1, we first compile the navigation program into LLVM IR and construct the DDG, where each node denotes only a useful instruction with its power consumption and each edge represents the data dependency with the weight being data size times latency. Second, based on DDG graph, we propose a scheduling algorithm to partition the PNI application into clusters such that (1) inter-cluster communication is minimized, (2) NoC energy is reduced and (3) the workloads of different cores are balanced for maximum parallel execution. Finally, we incorporate topological sort into the our energy-aware mapping scheme to further reduce static power consumption resulted by congestion.

Towards this end, the main contributions of this paper are as follow:

- To the best of our knowledge, our work is the first to incorporate the static energy consumption analysis of application into a compiler-based task partition.
- Besides volume, we propose a mapping strategy to also consider the timing of inter-core communications, reducing the congestion time and static energy consumption of hardware resources.

The rest of the paper is organized as follows: Section II discusses the related work. Section III introduces the basics of UAV control. Section IV illustrates the energy model for NoCs, the load-balancing and energy-aware community detection algorithm, and the low-power mapping. Section V validates the framework and shows experimental results compared to the baseline model.

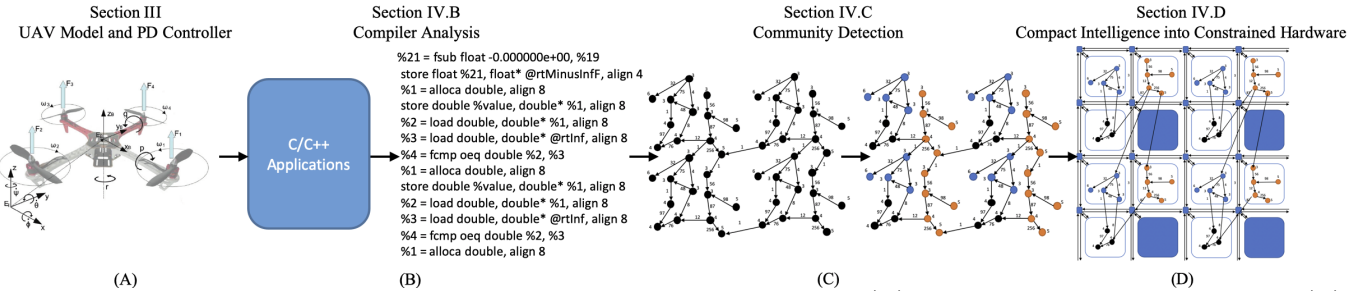


Fig. 1.: Overview of the UAV intelligent processing architecture workflow. (A): An UAV and its control basics. (B): The perception and navigation intelligence application (as a high level program) is compiled into LLVM IR trace through compiler analysis. This allows to remove the unnecessary computation and communication overhead of high level programs. (C): We transform the trace into the DDG and detect communities. (D): Each processing community is mapped onto an NoC processing element in such a way that its communication energy is minimized and congestion is reduced. The unused cores are clock-gated to save energy, indicated by the blue tiles.

II. RELATED WORK

There has been a significant amount of previous research on energy-aware and load-balancing scheduling and mapping on multicore embedded systems. From a mathematical and control perspective, Bogdan et al. in [4, 5] provide a complex approach to dynamically characterize the workload of multicore systems for performance and power optimization. Xiao et al. propose a complex network-inspired application partitioning tool to improve multicore parallelization [15]. Tan et al. develop a low-power customizable manycore architecture for wearables using a lightweight message-passing scheme [14]. Navion [13] design an energy-efficient accelerator to fully integrate visual-inertial odometry system-on-chip while eliminating expansive off-chip processing and storage for autonomous navigation of drones. In terms of mapping and routing, an efficient branch-and-bound algorithm proposed by Hu et al. [9] automatically maps the IPs onto a generic NoC so that the communication cost is minimized while the timing constraint is met. In contrast to prior work, we present an energy-aware load-balancing community detection algorithm together with a mapping strategy and test it using a UAV self-navigation application.

III. BRIEF OVERVIEW OF THE BASICS OF THE UAV NAVIGATION CONTROLLER

Fig. 1(A) shows a UAV with six degrees of freedom. Three degrees of freedom describe the translational motions (x, y, z) and the other three are the rotational motions (r, p, q). Each of the four propellers is equipped with a rotor providing the angular velocity. These four angular velocities correspond to the inputs of the quadrotor, $\omega_i = [\omega_1, \omega_2, \omega_3, \omega_4]$. Twelve outputs are generated from the quadrotor, $X = [x, y, z, r, p, q, \dot{x}, \dot{y}, \dot{z}, \dot{r}, \dot{p}, \dot{q}]$, corresponding to the translational and rotational positions, and their corresponding velocities [6].

For real-time applications, the error between the actual UAV position, estimated by a navigation system, and the desired position is fed into a PD-controller to determine the required control inputs. The required rotor speeds are

then calculated from the respective torques using:

$$\begin{pmatrix} T \\ \Gamma \end{pmatrix} = \begin{pmatrix} -b & -b & -b & -b \\ 0 & -db & 0 & db \\ -db & 0 & db & 0 \\ k & -k & k & -k \end{pmatrix} \begin{pmatrix} \omega_1^2 \\ \omega_2^2 \\ \omega_3^2 \\ \omega_4^2 \end{pmatrix} \quad (1)$$

where T is the thrust vector for each propeller, Γ is the torque vector applied to the airframe, b represents the lift constant, d is the distance from the rotor to the center of the mass and k is secondary lift constant. The control structure employed to fly the quadrotor can be found in [6, 2], and is based on Proportional Derivative action to get the quadrotor's attitude (roll, pitch, yaw) and altitude.

IV. PARALLELIZATION DISCOVERY AND ENERGY OPTIMIZATION APPROACH

A. Energy Model

Both IP cores and interconnection consume energy. While most of the mapping algorithms based on the one in [9] only compute dynamic energy, our model considers both static and dynamic power dissipation. N. Grech et al. [8] propose an application static energy analysis technique to determine the instruction energy model directly at the LLVM IR level. Through analysis and measurement of a large set of target ISA instructions, it was found that LLVM IR instructions can be divided roughly into four groups: memory, M , program flow, B , division, D , and all other instructions, G . This yields an energy model E_N of a program executed sequentially in a computing node:

$$E_N = \sum_{i \in \{M, B, D, G\}}^n E_i N_i \quad (2)$$

where E_i is the energy cost of a single instruction in group i , N_i is the number of the instructions executed in that group, and n denotes the number of instructions.

Using the bit energy concept proposed by Ye et al. in [16], the total dynamic energy consumption can be computed by:

$$E_{DyNoC} = \sum_{i=1}^a \sum_{j=1}^b w_{ij} (\eta_{ij} E_{S_{bit}} + (\eta_{ij} - 1) \times E_{L_{bit}}) \quad (3)$$

where $E_{S_{bit}}$ and $E_{L_{bit}}$ represent the energy consumed by switch and link; η_{ij} is the number of routers the packet from tile τ_i to tile τ_j passes through along the way; w_{ij} is the size of the packet; a and b denote the number of tiles on x and y respectively.

The static power is defined to characterize the energy consumed when packets are congested in the buffers. For simplicity, static power is defined as:

$$E_{StNoC} = \sum_{i=1}^n P_{St} \times w_i \times t_i \quad (4)$$

where n is the number of times that congestion occurs; P_{St} is the energy consumption of one bit of data stored in the buffer for one unit of time; w_i is the data size of the i th congestion; and t_i is time of the i th congestion. Equation (5) gives the total energy consumption for the interconnect.

$$E_{NoC} = E_{StNoC} + E_{DyNoC} \quad (5)$$

Finally, given the total number of tiles n , the energy consumption of the entire chip is computed as:

$$E = \sum_{i=1}^n E_{N_i} + E_{NoC} \quad (6)$$

B. Compiler Analysis and Model of Computation Extraction

In order to generate the data dependency graph (DDG), we adopt the LLVM IR [10]. The rationale behind this is that LLVM is a language-independent system that exposes the commonly-used primitives to implement high-level language features, which makes it very easy to generate back-end for any target platform.

With the help of Clang, C/C++ applications are compiled into a dynamic IR execution trace. We developed a parser to construct a data dependency graph from the IR trace. The parser analyzes memory operations to obtain latency and data sizes. Because the execution times and energy vary on data sizes and where the data resides, taking those values into account could potentially reduce inter-core communications by grouping the source and destination instructions of a register into one cluster. Three hash tables are created and updated when parsing: the source table, the destination table and the dependency table. The source/destination tables are used to keep track of source/destination registers with keys being source or destination registers and values being the

TABLE I
: The source, destination and weight tables

LLVM IR trace					
store double %5, double* %1, align 8 %2 = load double, double* %1, align 8 %3 = load double, double* %6, align 8 %4 = fcmp oeq double %2, %3					
Src Table Dest Table Dependency Table					
Key	Value	Key	Value	Key	Value
%5	1	%1	1	2	1
%1	2	%2	2	4	2,3
%6	3	%3	3		
%2, %3	4	%4	4		

corresponding line number. The dependency table is to store dependencies between nodes with keys being the line number for current instruction, and values being clock cycles, data sizes and line numbers of previous instructions dependent on the same virtual register.

For example, in Table I, a LLVM IR snippet is extracted from an application compiled by Clang front-end. As the parser reads the first line, a source table and a destination table are created. The source table is updated with the key being %5 and the value being 1 and its destination register is hashed into the destination table with the key being %1 and value the being 1. When line 2 is read, the source register %1 happens to be the destination register in line 1. A dependency table is created and updated with the key being 2 (line number of current instruction) and value being 1 (line number of the dependent instruction). Following the same procedure, the three hash tables will look like what is shown in Table I.

C. Discovering the Processing Community Structure

To formulate this problem, we introduce the following concepts:

Definition 1. A data dependency graph (DDG) is a weighted directed graph $G = G(a_i, b_{ij}, e_i, w_{ij} | i, j \in N|)$ where each vertex a_i represents one LLVM IR instruction; each edge b_{ij} with weights w_{ij} characterizes either the dependency from a_i to a_j or the control flow such as jumps or branches from one block to another; and e_i stands for the estimated energy of the vertex given in Section IV.A.

Definition 2. A weight w_{ij} between a_i and a_j is calculated by latency times data size. Latency characterizes the delay from a_i to a_j based on the timing information. Data size represents the number of bytes transferred.

Definition 3. A quality function determines how efficient the LLVM IR instructions are grouped together in terms of energy consumption, parallelism, load balancing, hardware utilization and inter-cluster data movements.

The discovery of the processing community structure problem can now be formulated as follows: **Given**

a DDG, **find** non-overlapping processing communities which **maximize** the quality function:

$$Q = \sum_{c=1}^{n_c} \left(\frac{(W_c - S_c)}{W} - \frac{(W_c - \bar{W})^2}{W} \right) - \frac{\sum_{c=1}^{n_c} E_{N_c} + E_L}{E} \quad (7)$$

and satisfy:

$$N \geq n_c \quad (8)$$

The first term in equation (7) confines the data flow within the cluster as much as possible. It indicates the difference between the sum of the weights in a cluster and the sum of the weights of the edge connected to the cluster. The greater this term is, the fewer inter-cluster data movements, and the more energy is saved.

The second term in equation (7) measures the standard deviation squared between sum of weights in cluster c and average sum of weights in all clusters. Minimizing this term ensures load balancing and fully takes advantage of parallel execution.

The third term in equation (7) characterizes the energy model of the application, where E_{N_c} calculates the energy consumed at each node using Equation (2) and E_L computes the energy consumption for communication transactions. To maximize quality Q , this term needs to be minimized in order to save energy.

D. Compact Intelligence Mapping into Constrained Hardware

The tile to which each cluster is mapped significantly affects the power consumption of the application since it determines the dynamic and static communication cost. Consequently, an approach, which is similar to the one in [9], is proposed, but it takes cluster ordering into consideration as well so that it reduces static energy consumption caused by congestion and contention of hardware resources.

Definition 4. A task graph (TG) is a weighted directed acyclic graph $TG = G(c_i, a_{ij}, v(a_{ij}), b(a_{ij}) | i, j \in N|)$ where each vertex c_i represents a cluster of LLVM IR instructions that are grouped together by our community detection algorithm, and each edge a_{ij} represents communication from node c_i to node c_j .

- $v(a_{ij})$: data size from c_i to c_j .
- $b(a_{ij})$: bandwidth requirement from c_i to c_j .

Definition 5. An architecture graph (AG) is a directed graph $AG = G(t_i, p_{ij}, e(p_{ij}) | i, j \in N|)$ where each vertex t_i represents a tile, and each edge p_{ij} represents a routing path from t_i to t_j .

- $e(p_{ij})$: energy consumption from t_i to t_j .
- $L(p_{ij})$: set of links that makes up p_{ij}

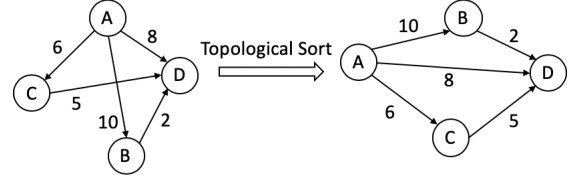


Fig. 2.: Application of a topological sort to task graph.

In order to exploit parallelism and pipelining, we apply topological sort to the task graph before mapping. The depth of cluster c_i is defined as the maximum number of edges from the root to c_i . In Fig. 2, cluster D cannot execute before cluster B and C because it needs data from both of them. However, cluster B and C can execute in parallel because they are at the same depth.

Algorithm 1: Compact Intelligence Mapping Algorithm

Input: TG and AG
Output: Mapping from TG to AG

```

1 count = 0
2 while  $TG$  is not empty do
3   if  $count == 0$  then
4     Get the cluster with depth of zero and map to
      (0,0)
5   else
6     Create a set  $S_{count}$  of all clusters with depth
      of  $count$ ;
7     Map  $S_{count}$  to the available tile in  $AG$  so that:
8      $\min\{E = \sum_{\forall a_{ij}} v(a_{ij})e(p_{map(c_i),map(c_j)})\}$ 
9    $count++$ 
10  if Any idle tile  $t$  left in  $AG$  then
11    Power gate  $t$ 

```

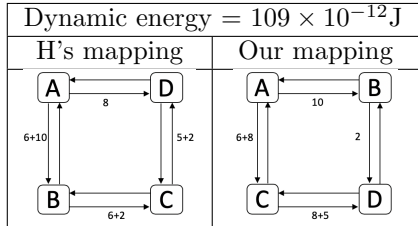
D.1 Energy and Congestion Analysis

The energy-aware mapping proposed in [9] (we refer to it as H) fails to consider the order of the clusters, leading to significant potential congestion and static energy consumption in NoCs. This section shows how our algorithm mitigates this problem.

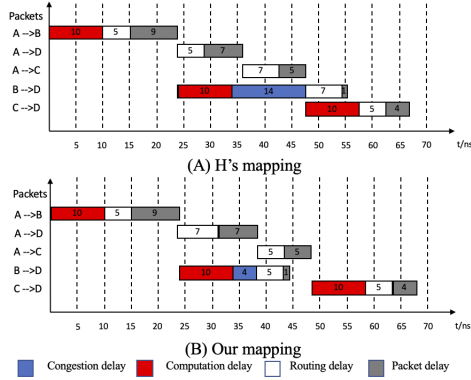
For illustration purposes, we assume $E_{S_{bit}} = E_{L_{bit}} = 1 \times 10^{-12} J/bit$. Applying the H's mapping to the TG in Fig. 2 may yield the following two different mappings in Table 2. For instance, using Equation (3) in H's mapping, $E_{DyAC} = 6 \times (3 \times E_{S_{bit}} + (3 - 1) \times E_{L_{bit}}) = 30 \times 10^{-12} J$. Both mappings' dynamic energy costs are $109 \times 10^{-12} J$.

In terms of static energy, we assume $P_{St} = 1 \times 10^{-12} J$, and the execution time is $10ns$ for all clusters. Also assume one packet flit is $1bit$ and the time for a flit to pass through a switch (t_s) is $2ns$ and a link (t_l) is $1ns$. Fig. 3 shows the timing diagram of all computations and all packet deliveries of both mappings. For instance, in H's mapping, the first flit of the packet from cluster A to B

TABLE II
: Mapping comparison: dynamic energy



takes $2 \times t_s + t_l = 5 \text{ns}$ to arrive (routing delay), while the rest of the packet needs another 9ns (packet delay).



In H's mapping, when cluster B finishes execution and is about to route the packet to D , D 's input buffer is busy because of $A \rightarrow D$ and $A \rightarrow C$ packet transmissions. Thus, B must wait until $A \rightarrow C$ is done. While the two mappings yield the same execution time of 67ns , the packets from B to D in H's mapping experiences a 10ns longer congestion delay, hence consuming more static energy. Applying Equations (4) and (5), H's mapping consumes 17% more energy in interconnect.

V. EXPERIMENTAL RESULTS

We use gem5 [3] together with McPAT [11] for architectural and power simulation. Our baseline model is 2-core ARM processor connected in a 2D mesh topology NoC [1] with MESI cache protocol. Detailed parameters are listed in TABLE III.

TABLE III
: Simulation parameters of baseline processor

Cores	2 in-order ARM cores at 500MHz
L1 Private Cache	32KB, 4-way, 32-byte block
L2 Shared Cache	128KB, 8-way
Topology	2D Mesh with XY routing

First, we examine our processing community discovery algorithm's computational complexity (Fig. 4) as the number of core grows. The processing community discovery is done offline (only once), so a run time around two minutes will not affect the controller speed during UAV navigation. For system sizes under 256, the run time is roughly only related to the map size and remains constant

as the core number increases. Once the core count passes a threshold of 256, the run time rises significantly.

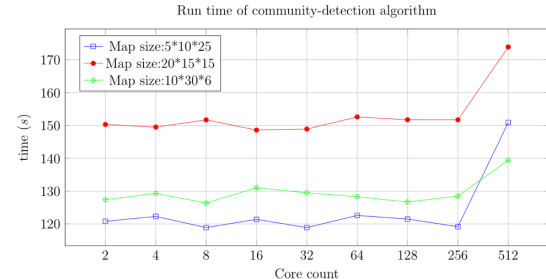


Fig. 4.: Run-time of community detection algorithm.

TABLE IV
: TGs of different core count

Row	#Core	Inst/core (SD)	(Inter-core) flits	Avg degree	Avg weight
1	1	16637	24324	2.31	13.87
2	BL	514.9	12023	2932	15.87
3	2	415.9	8497	2646.5	11.48
4	4	199.6	6391	1932.2	12.64
5	8	104.8	4213	748.5	11.88
6	16	53.2	3531	593.5	10.67
7	32	29.1	2919	713.8	9.73
8	64	12.5	1823	293.3	10.58
9	128	13.4	3769	252.9	7.84
10	256	7.3	5322	120.3	12.39
11	512	4.3	14483	45.9	16.99

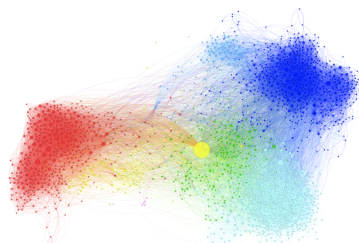


Fig. 5.: DDG of UAV navigation application.

The statistics of the generated clusters are shown in TABLE IV. The row 1 in the Inst/core (SD) column stands for the total number of instructions of this application; starting from row 2, it records the standard deviation of the number of instructions partitioned into each cluster. The row 1 in the (Inter-core) flits column stands for the total number of edges in this application; starting from row 2, it records the total number of flits needed to be transported between cores. The baseline is randomly partitioned. As the number of cores increases, the inter-core communication first drops to 913 (86.4% reduction compared to the baseline) edges at 64 cores and then soars to 7482 at 512 cores (11.3% more than baseline). Same on 2 cores, our algorithm reduces the edges by 21.2%. The reason is that our algorithm effectively lowers the inter-core communication when the core count is less than 64. After

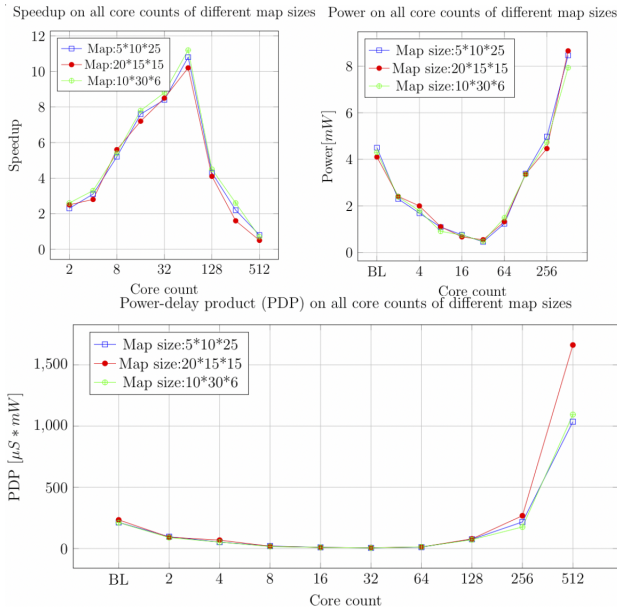


Fig. 6.: Speedup, power and PDP of different core counts. 64, as fewer and fewer instructions are run on each core, the inter-core message passing increases dramatically.

Next, we evaluate the speedup and power consumption of our design (Fig. 6). The power values are collected by feeding the outputs from gem5 to McPAT. Having fully taken advantage of parallel execution, load-balancing and optimal inter-community communication, our design has achieved maximum speedup of around 10.5x at 64-core architecture and energy savings of 8.4x at 32 cores. The scalability of this application is roughly under 64 cores due to the relatively small number of instructions. Mapping to 512 cores even yields longer run times and higher energy consumption because more flits need to be routed between cores. The delay in Fig. 6 refers to the time to run one iteration of the next target position calculation. The minimum power-delay product is achieved by the 32-core configuration at $5.56\mu S * mW$, 39.3x lower than the baseline power delay product (PDP) of $219.6\mu S * mW$. It is noted that map size hardly affects the run time and power, as simulations run on three different map sizes are approximately the same.

TABLE V

: Power consumption of DJI flight controllers

Model	Max Power	Normal Power
DJI ACE ONE	5W	3.2W
DJI NAZA-H	3.2W	1.5W
DJI NAZA-M LITE	1.5W	0.6W
DJI NAZA-M V2	1.5W	0.6W

Finally, we illustrate the potential of our design by comparing it with the state-of-art flight controllers used in DJI drones. As shown in Table V, NAZA-M LITE has the lowest power consumption among the other controllers with a max power of 1.5W and a normal power of 0.6W. Our design consumes significantly less energy compared to the DJI's controllers.

VI. CONCLUSION

In this paper, we first develop an LLVM IR parser to construct the DDG for UAV autonomous navigation application. Next, we analyze the DDG structure and discover its best parallelization degree by applying our load-balancing and energy-aware processing community discovery algorithm so that data movement is confined within clusters and static energy consumption is minimized. Finally, a congestion-aware mapping scheme based on topological sort is proposed to map clusters onto the NoCs for parallel execution. Simulations show that our optimal 32-core design achieves an average 8.4x energy savings and that 64-core configuration achieves 10.5x performance speedup.

REFERENCES

- [1] N. Agarwal, T. Krishna, L.-S. Peh, and N. K. Jha. Garnet: A detailed on-chip network model inside a full-system simulator. In *2009 ISPASS*, pages 33–42. IEEE, 2009.
- [2] S. Armah, S. Yi, W. Choi, and D. Shin. Feedback control of quad-rotors with a matlab-based simulator. *American Journal of Applied Sciences*, 2016.
- [3] N. Binkert, B. Beckmann, G. Black, S. K. Reinhardt, A. Saidi, A. Basu, J. Hestness, D. R. Hower, T. Krishna, S. Sardashti, et al. The gem5 simulator. *ACM SIGARCH Computer Architecture News*, 39(2):1–7, 2011.
- [4] P. Bogdan. Mathematical modeling and control of multifractal workloads for data-center-on-a-chip optimization. In *Proceedings of the 9th NOCS*, page 21. ACM, 2015.
- [5] P. Bogdan and Y. Xue. Mathematical models and control algorithms for dynamic optimization of multicore platforms: A complex dynamics approach. In *Proceedings of the ICCAD*, pages 170–175. IEEE Press, 2015.
- [6] P. Corke. *Flying Robots Book: Robotics, Vision and Control*. Springer, 2017.
- [7] W. J. Dally and B. Towles. Route packets, not wires: on-chip interconnection networks. In *Proceedings of the 38th DAC*, pages 684–689. Acm, 2001.
- [8] N. Grech, K. Georgiou, J. Pallister, S. Kerrison, J. Morse, and K. Eder. Static analysis of energy consumption for llvm ir programs. In *Proceedings of the 18th SCOPES*, pages 12–21. ACM, 2015.
- [9] J. Hu and R. Marculescu. Exploiting the routing flexibility for energy/performance aware mapping of regular noc architectures. In *2003 DATE*, pages 688–693. IEEE, 2003.
- [10] C. Lattner and V. Adve. Llvm: A compilation framework for lifelong program analysis & transformation. In *Proceedings of the CGO'04*, page 75. IEEE Computer Society, 2004.
- [11] S. Li, J. H. Ahn, R. D. Strong, J. B. Brockman, D. M. Tullsen, and N. P. Jouppi. Mcpat: an integrated power, area, and timing modeling framework for multicore and manycore architectures. In *Proceedings of the 42nd MICRO*, pages 469–480. ACM, 2009.
- [12] T. H. Natalie Kitroeff. Boeing's 737 max suffers setback in flight simulator test, 2019
- [13] A. Suleiman, Z. Zhang, L. Carlone, S. Karaman, and V. Sze. Navion: A 2-mw fully integrated real-time

visual-inertial odometry accelerator for autonomous navigation of nano drones. *IEEE Journal of Solid-State Circuits*, 2019.

- [14] C. Tan, A. Kulkarni, V. Venkataramani, M. Karunaratne, T. Mitra, and L.-S. Peh. Locus: Low-power customizable many-core architecture for wearables. *TECS*, 17(1):16, 2018.
- [15] Y. Xiao, Y. Xue, S. Nazarian, and P. Bogdan. A load balancing inspired optimization framework for exascale multicore systems: A complex networks approach. In *Proceedings of the 36th ICCAD*, pages 217–224. IEEE Press, 2017.
- [16] T. T. Ye, L. Benini, and G. De Micheli. Analysis of power consumption on switch fabrics in network routers. In *Proceedings 2002 DAC*, pages 524–529. IEEE, 2002.